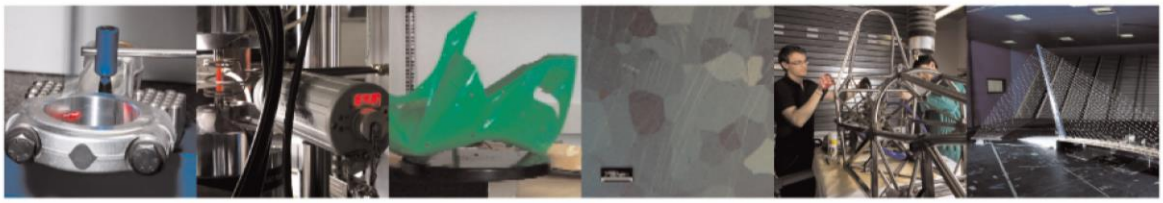

Tolerance analysis of gear trains by static analogy

Antonio Armillotta

This is a post-peer-review, pre-copyedit version of an article published in Mechanism and Machine Theory. The final authenticated version is available online at: http://dx.doi.org/10.1016/j.mechmachtheory.2019.01.029]

DIPARTIMENTO DI MECCANICA ■ POLITECNICO DI MILANO
via G. La Masa, 1 ■ 20156 Milano ■ EMAIL (PEC): pecmecc@cert.polimi.it
http://www.mecc.polimi.it
Rev. 0

Tolerance analysis of gear trains by static analogy

Antonio Armillotta

Politecnico di Milano, Dipartimento di Meccanica
Via La Masa 1, 20156 Milano, Italy
Tel.: +39-02-23998296
Email: antonio.armillotta@polimi.it

Abstract

Assembly-level geometric errors such as backlash, center distance errors and shaft misalignments may adversely affect the operation of a gear train. The tolerance analysis method proposed in the paper estimates these errors from tolerance specifications on gears and mounting parts (shafts, bearings, housings). The problem is solved by analogy with an equivalent problem of force analysis: on a properly defined structure, external forces correspond to the assembly-level error, and calculated internal forces and support reactions provide the sensitivities of part tolerances on the total error. Previously developed for generic assemblies, the approach proves especially simple for gear systems compared to existing methods of tolerance analysis, as it relies upon structural analysis procedures that are customary in mechanical design. The method based on static analogy includes a two-level classification of geometric errors, which helps overcome the complexity of tolerance analysis problems for gearings. Two examples of gear trains of different types and configurations are presented to demonstrate the calculation procedure and verify its correctness by comparison with geometric considerations.

Keywords: Gears, statistical tolerancing, force analysis

1 Introduction

Any mechanical device has to meet functional requirements, i.e. precision-related conditions for assemblability, durability and operational performance. A requirement is associated with a geometric key characteristic involving different parts of the assembly; its variation cannot be inspected during the manufacturing process, as it results from the stackup of tolerances on individual parts. Tolerance analysis estimates the errors on a functional requirement from the deviations allowed on part features, defined as either worst-case limits or statistical distributions. Several methods, reviewed in [1, 2, 3], are available for this task under different sets of assumptions.

Mechanisms involve special difficulties in tolerance analysis. They tend to have many parts in mutual contact along different directions, and their degrees of freedom can cause displacements of contact points due to internal forces. As a result, functional requirements and part dimensions are not usually related by simple mathematical equations. This paper deals with gear trains, which raise all the above issues and may come in widely different configurations, even if based on similar part types (gears, shafts, bearings, housings) and on a typical functional scheme (transmission of rotary motion between two end shafts).

Tolerance specifications on gears are discussed in specialized technical literature, e.g. [4]. The importance of functional requirements such as backlash and transmission error is pointed out for applications in instruments and control systems. Traditionally, the errors on these characteristics were almost exclusively measured through direct procedures based on master gears [5]. More recently, coordinate measuring machines have allowed an easier inspection of the active surfaces of gear teeth [6, 7], giving an impulse to the evolution of geometric specifications and related standards [8, 9, 10]. Therefore, there is a growing need for computational methods for estimating the variation of functional requirements from specified tolerances.

On a meshing pair, geometric errors influence the actual contact conditions between gear teeth causing deviations from correct kinematic and static behavior. Tooth contact analysis simulates such effects from

assumptions or measured data on tooth geometry. Initially, a differential-geometry model was built on involute profile equations [11] and implemented as a simulation tool for estimating transmission error [12, 13, 14]. The approach has been extended to different gear types [15, 16], and the discretization of tooth surfaces has allowed meshing simulation from either mathematically generated deviations [17] or point clouds collected from actual gears [18].

Tooth contact analysis has later been integrated into methods for the statistical analysis of geometric tolerances in accordance with international standards. In [19, 20, 21], a vectorial tolerancing model of geometric specifications is used to generate random error variables in the transformation matrices associated with tooth contacts, allowing a Monte Carlo simulation of transmission error. The concept of skin model shapes is adopted in [22, 23, 24], where deviations from nominal tooth profile are generated by random fields on discretized geometric models of the gears; interference detection algorithms on such models allow us to simulate gear meshing and estimate transmission error, with validation through measured data. A related topic is the evaluation of the dynamic effects of geometric errors, carried out by different methods in [25, 26, 27, 28].

When dealing with gear trains, simulating all meshes may become impractical, while additional error sources are to be considered, such as the eccentricities of mounting surfaces on gears and other parts of the transmission. An early procedure for the analysis of backlash and transmission error for spur gears was proposed in [5]: for each tolerance type, e.g. diameter, runout or profile, an individual contribution to the total error is calculated by equations deriving from geometric considerations; the contributions are then linearly combined with both worst-case and statistical approaches. In [29], functional errors are similarly estimated by solving linear systems of equations developed for different gear types.

While the above methods associate a fixed contribution to each type of tolerance, the layout of the gear train may influence the impact of geometric errors; for example, the same position error on a support bore may cause different mesh eccentricities depending on how far the support is located from gears and other supports. Such effects could be better captured by existing methods for the tolerance analysis of other types of mechanisms. The direct linearization method has first been developed for generic assemblies [30, 31], then adapted to mechanisms [32], and recently extended to deal with overconstraining and part compliance [33, 34]. Other methods express part relations by explicit equations, which lead to Monte Carlo simulation of assembly errors [35, 36] or to probabilities of violating correct operational conditions [37, 38].

The specific geometry and working principle of gearings might call for an alternative approach, referred to as kinematic tolerance analysis, where errors on key characteristics of mechanisms (e.g. drive ratio, backlash, and jerk) are calculated with the help of known procedures of kinematic analysis. Early methods were based on Monte Carlo simulation [39, 40, 41]; formulations with improved efficiency have later been developed based on the concept of configuration space [42, 43, 44]. An application of this approach to a gear mechanism is reported in [45] without details on mesh kinematics. Further methods have been proposed for robotic manipulators, where joint clearances create additional difficulties to the analysis of kinematic errors. These are treated by defining additional entities (virtual links) in existing models including the vector loop [46], Denavit-Hartenberg equations [25, 47, 48], and the screw theory [49, 50, 51, 52].

In this paper, the tolerance analysis of gear trains will be carried out by a method based on an analogy with force analysis problems. The potential advantage of this approach is the opportunity of doing tolerance calculations by using known procedures of statics as well as computer-aided tools for structural analysis. The static analogy has been proposed in [53] as an application of the principle of virtual work of rigid bodies, and later applied to mechanisms and exactly constrained assemblies [54]. A few other approaches relying on statics are available in literature for the tolerance analysis of manipulators [55, 56, 57, 58, 59]. The links between tolerance analysis and statics have also been recognized for overconstrained and compliant assemblies, where stress analysis is needed to evaluate the deformations induced at assembly stage. In this context, the method of influence coefficients [60] is praised to allow an especially efficient use of finite-element solvers, which reduces or completely avoids the need for Monte Carlo simulation.

In principle, the static analogy is applicable to any type of assembly after a careful definition of the static model equivalent to the specific tolerance analysis problem. For gear trains, such task is more difficult due to the high number and diversity of part features that are related to the functional requirements of interest. The need to simplify the static model as much as possible has led to an original approach based on a hierarchy of geometric errors. A first level defines composite errors at significant sections of the gear train, which are evaluated by analogy with simple beam systems. The second level breaks down each composite error as the sum of errors on coaxial part features located at the same section. The approach has been developed into an original method of tolerance analysis for gear trains, which is the main contribution of the present work.
Section 2 recalls the static analogy for generic mechanical assemblies. Section 3 describes the proposed method for gear trains, which is demonstrated on a basic example in Section 4. Calculation results are presented in Section 5, and further application details are illustrated in Section 6. The conclusions in section 7 discuss the potential of the method.

2 Static analogy

Tolerance analysis estimates the error δy on a functional requirement y from the errors δx_i on n dimensions x_i of part features that are thought to influence it. Errors are usually much smaller than dimensions, so their stackup is approximately linear:

$$\delta y \approx \sum_{i=1}^{n} s_i \delta x_i \,, \quad s_i = \frac{\partial y}{\partial x_i}$$

In cases of realistic complexity, an explicit equation $y = f(x_1, \ldots, x_n)$ is unavailable and the sensitivities s_i have to be evaluated from part geometry and assembly relations. This is done differently by existing methods in literature. In the method based on static analogy [53, 54], the requirement y is associated with a force F, which is applied as an external load to the assembly. After solving this static model, regarded as equivalent to the tolerance analysis problem, the sensitivities are calculated as

$$s_i = \frac{F_i}{F}$$

where F_i is a support reaction or an internal force, properly chosen in association with x_i. A justification of this result has been proposed by considering errors δx_i and δy as virtual displacements of the points where F_i and F act, then noting that the error stackup model corresponds to the equality of the virtual works of internal and external forces, which is an equilibrium condition for the system.
In previous papers [53, 54], the static analogy was applied to several examples of assemblies and mechanisms, in order to clarify how the static model can be built in different cases. The main choices are summarized below:

- The load F is defined according to the type of requirement to be analyzed. If the requirement is a linear (angular) distance between two features, the load includes two opposing forces (torques) acting on the two features in the same direction of the distance (angle).
- The reactions or internal forces F_i are associated to the different part features according to few basic rules. A distance corresponds to a normal force between two points or planes (positive if tensile, negative if compressive). An angular position correspond to a bending moment (positive or negative with the same convention of the angle). A radius corresponds to a sum of radial forces acting on the circle (positive if directed outwards, negative if directed inwards). In a cylindrical fit, the diameters of the two features correspond to half the contact force (positive for the hole, negative for the shaft).

In [53], the correctness of the static analogy was verified on simple examples by comparison with geometric reasoning, graphic procedures, and the direct linearization method [30] widely used in tolerance analysis. Even without a full validation, it is expected that in general cases the static analogy would provide roughly the same results as existing methods. Compared to these, a possible advantage is the use of well-established

calculation procedures such as the force analysis of free body diagrams, reducing the need for special types of abstract models (such as the vector loop in the cited method).

3 Main approach

The proposed method analyzes the variation on given functional requirements for a gear train. The paper mainly deals with compound gear trains consisting of spur or helical gears; with minor extensions, however, the same calculation procedures are applicable to bevel gears or planetary gear trains. The functional errors usually considered for gear trains include:

- linear and angular misalignments between end shafts (Fig. 1a);
- deviations on nominal center distances of meshing gears (fig. 1b);
- angular backlash at the output shaft (fig. 1c).

These errors are assumed to depend only on the manufacturing errors on part features, without considering additional variation sources such as thermal expansion and deflections due to operating loads. Angular mounting positions of meshing gears are assumed to be random without any runout-compensating adjustment.

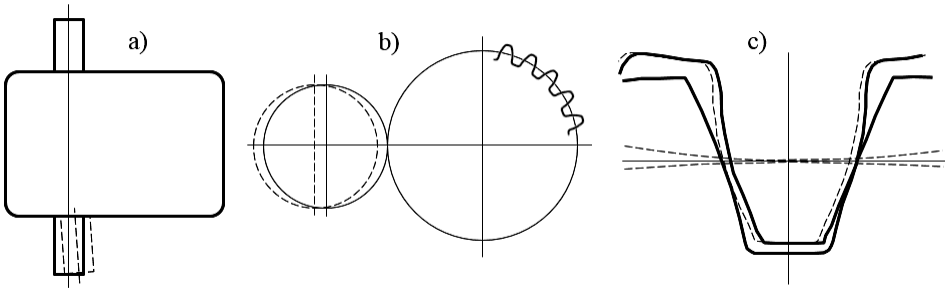

Fig. 1: Types of functional requirements: a) shaft alignment, b) center distance, c) backlash

3.1 Data

A gear train generally includes gears, shafts, bearings and housings. All types of parts have an influence on functional errors, along with possible other ones (keys, seals, etc.) that will not be considered in this work. Some part dimensions are needed for the analysis; these include the pitch diameters of the gears, and the axial positions of the sections where the gears and the bearings are mounted on the shafts.

The tolerances specified on the parts of the gear train must also be collected for the analysis. In general, the features of interest include external cylinders (shaft journals, bearing outer rings), and internal cylinders (gear bores, bearing inner rings, housing bores). Each feature is assumed to have a diameter tolerance and a positional tolerance with respect to given datum features (bores of gears and bearings, journal pairs of shafts, external mating features of the housing). The gears are assumed to have no profile shifting and to be toleranced on pitch circle runout, tooth thickness and tooth profile.

The above tolerances can be classified into four types:

- diameter tolerances on journals and bores: as a general notation, the error δ on an outside diameter is limited by a tolerance T_d ($-T_d/2 \le \delta \le T_d/2$), while the error Δ on an inside diameter is limited by a tolerance T_D ($-T_D/2 \le \Delta \le T_D/2$);
- positional tolerances on journals and bores and on the pitch circles of gears; the radial displacement ε of the axis of a cylindrical feature is limited by a tolerance T_e ($-T_e/2 \le \varepsilon \le T_e/2$);
- tooth thickness tolerances ($-T_t/2 \le \tau \le T_t/2$);
- tooth profile tolerances, defined along the pitch circle arc ($-T_E/2 \le \eta \le T_E/2$).

The positional tolerances may control different characteristics depending on whether the feature is a toothed surface (pitch circle runout), a journal (coaxiality to other journals), a bore (coaxiality and center distance),

or a bearing outer ring (radial play and coaxiality to the inner ring). Each error is assumed to be normally distributed with zero mean and standard deviation σ in a fixed relationship with the tolerance, e.g. $T = \pm 3\sigma$.

3.2 Static model and composite errors

According to the static analogy, a problem of tolerance analysis requires the solution of an equivalent problem of force analysis. In a gear train, forces are decomposed into radial, tangential, and axial components. Each type of force component will provide the sensitivities of different types of tolerances:

- radial forces correspond to diameter and positional tolerances, which cause radial eccentricities;
- tangential forces correspond to tooth thickness and profile tolerances, which cause displacements along the pitch circle arcs of gears;
- axial forces correspond to positional tolerances of axial features (e.g. shaft sleeves), which cause axial displacements that may be relevant for helical or bevel gears.

A gear train has to be described by a static model, i.e. a simplified representation suitable to force analysis. For general assemblies, the static model is a system of rigid parts connected through mating features; the difficulty of static calculations depends on the degree of constraining and on the types of mating relations. If correctly designed and operated, a gear train is statically determinate due to the clearances between meshing teeth. Moreover, the free-body diagrams for gears and bearings of a gear train share a typical configuration: these parts can be regarded as hollow cylinders subject to opposing radial forces, one directed inwards on the outer diameter, the other directed outwards on the inner diameter. Therefore, the minimum complexity for the static model for a gear train can be achieved by considering only the shafts as representative of the whole set of parts: these correspond to a skeletal structure of beams subject to bending (radial), twisting (tangential), and normal (axial) forces. The beams are loaded or supported at points corresponding to the mounting sections of gears and bearings.

The above choice is equivalent to clustering the errors of all the parts at the same section i into a composite error e_i, which is the displacement of the corresponding point of the structure. As the structure can deform along different directions (radial, axial, tangential), each section may be associated to multiple composite errors. Each composite error has a composite sensitivity s_i.

3.3 Force analysis and breakdown of composite errors

To analyze a functional requirement, the skeletal structure is loaded by a suitable force or torque. The support reactions are calculated for each beam by appropriate equilibrium equations in translation and rotation. As a result, each point of the structure is associated with a force (load or reaction); the composite sensitivity at the point results from dividing the force by the load intensity.

Each composite error is related to the manufacturing errors on the part features located at the corresponding section. By extending the results already discussed for cylindrical fits, the sensitivity of a feature is calculated by multiplying the composite sensitivity by an appropriate factor depending on feature type:

- 1/2 for inside diameters;
- −1/2 for outside diameters and tooth thicknesses;
- 1 for positional and profile errors.

4 Reference case

An example will now be presented to demonstrate the steps of the procedure, to check some results by geometric reasoning, and to highlight useful properties for handling different cases.

4.1 Assembly layout and data

The compound gear train in the schematic drawing of Fig. 2 includes four spur gears: pinion 1 integral to the input shaft, gears 2 and 3 mounted on intermediate shaft 5, and gear 4 mounted on output shaft 6. Bearing

sets 7-8, 9-10 and 11-12 supporting the three shafts are fit to bores in housing 13; for demonstration purposes, different bearing arrangements have been chosen for the three shafts even if possibly non-optimal for rigidity and space saving. Some axial dimensions are defined at selected shaft sections (A, B,…, N); to simplify calculations, they are standardized into three types: length a of end journals on shafts, distance b between gears and bearings, and distance c between bearings. The gears have pitch circle radii r_1, r_2, r_3 and r_4, which satisfy the condition for a reverted gear train ($r_1 + r_2 = r_3 + r_4$).

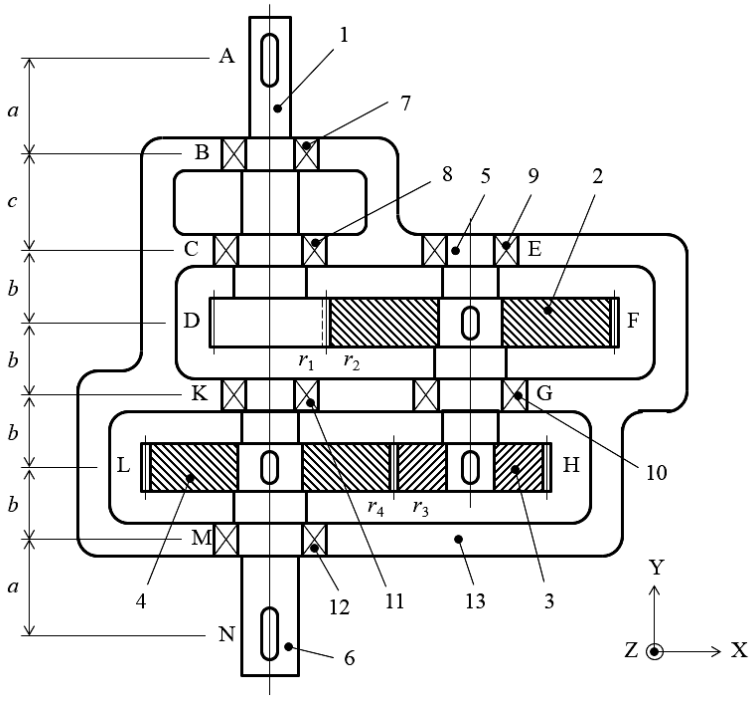

Fig. 2: Example of gear train

Tab. 1 lists the geometric errors for which tolerances are specified on the parts of the gear train. These are named with reference to the parts (1, 2, … 13) and the shaft sections where they are located (A, B,…, N). Bearing inner rings and corresponding shaft journals are not included in the list because they are press-fit datum features, whose deviations do not create radial clearance or runout.

4.2 Composite errors

For the gear train in Fig. 2, the static model is a system of three beams corresponding to the input, intermediate and output shaft. Under the loads corresponding to the different functional requirements, the beams will be subjected to only radial forces (along direction X) and tangential forces (along direction Z); there will be no axial forces (along direction Y), as the assembly does not include helical or bevel gears.
The radial forces will correspond to a first subset of composite errors (e_A, e_B, … e_N), each related to the X coordinate of a different point of the structure. The tangential forces will correspond to a second subset of composite errors (e_1, e_2, e_3, e_4), each representing the deviation on the pitch point of a different gear along direction Z. This leads to the following set of composite sensitivities:

$$\mathbf{S} = \{s_A, s_B, \ldots, s_N, s_1, \ldots s_4\}$$

For each functional requirement, the composite sensitivities will be evaluated by force analysis of the static model under a suitable load. As a last step, the sensitivities of part features will be calculated from the composite sensitivities by applying the factors listed in Section 3. To help this task, Tab. 2 expresses each composite error as an algebraic sum of feature errors, so that the related factor could be readily calculated as a derivative. For example, the error on the bore diameter of gear 2 will have the following sensitivity:

$$s(\Delta_{2F}) = s_F \cdot \partial e_F / \partial \Delta_{2F} = s_F / 2$$

Tab. 1: Geometric errors on the parts of the gear train

Part	*Section*	*Errors*	*Description*
1	A	ε_{1A}	Shaft 1, end section: coaxiality to support journals
	D	ε_{1D}, τ_{1D}, η_{1D}	Shaft 1, pinion: coaxiality to support journals, tooth thickness and profile
2	F	Δ_{2F}, ε_{2F}, τ_{2F}, η_{2F}	Gear 2: bore diameter, pitch circle coaxiality to bore, tooth thickness and profile
3	H	Δ_{3H}, ε_{3H}, τ_{3H}, η_{3H}	Gear 3: bore diameter, pitch circle position, tooth thickness and profile
4	L	Δ_{4L}, ε_{4L}, τ_{4L}, η_{2L}	Gear 4: bore diameter, pitch circle position, tooth thickness and profile
5	F	δ_{5F}, ε_{5F}	Intermediate shaft 1, journal for gear 2: diameter and position
	H	δ_{5H}, ε_{5H}	Intermediate shaft 2, journal for gear 3: diameter and position
6	L	δ_{6L}, ε_{6L}	Output shaft 6, journal for gear 4: diameter and coaxiality to support journals
	N	ε_{6N}	Output shaft 6, end section: coaxiality to support journals
7	B	δ_{7B}, ε_{7B}	Bearing 7, outer ring: diameter and coaxiality to inner ring
8	C	δ_{8C}, ε_{8C}	Bearing 8, outer ring: diameter and coaxiality to inner ring
9	E	δ_{9E}, ε_{9E}	Bearing 9, outer ring: diameter and coaxiality to inner ring
10	G	δ_{10G}, ε_{10G}	Bearing 10, outer ring: diameter and coaxiality to inner ring
11	K	δ_{11K}, ε_{11K}	Bearing 11, outer ring: diameter and coaxiality to inner ring
12	M	δ_{12M}, ε_{12M}	Bearing 12, outer ring: diameter and coaxiality to inner ring
13	B	Δ_{13B}, ε_{13B}	Housing 13, bore for bearing 7: diameter and position to datum reference frame
	C	Δ_{13C}, ε_{13C}	Housing 13, bore for bearing 8: diameter and position to datum reference frame
	E	Δ_{13E}, ε_{13E}	Housing 13, bore for bearing 9: diameter and position to datum reference frame
	G	Δ_{13G}, ε_{13G}	Housing 13, bore for bearing 10: diameter and position to datum reference frame
	K	Δ_{13K}, ε_{13K}	Housing 13, bore for bearing 11: diameter and position to datum reference frame
	M	Δ_{13M}, ε_{13M}	Housing 13, bore for bearing 12: diameter and position to datum reference frame

Tab. 2: Composite errors

Error	*Expression*
e_A	ε_{1A}
e_B	$-\delta_{7B}/2 + \varepsilon_{7B} + \Delta_{13B}/2 + \varepsilon_{13B}$
e_C	$-\delta_{8C}/2 + \varepsilon_{8C} + \Delta_{13C}/2 + \varepsilon_{13C}$
e_D	ε_{1D}
e_E	$-\delta_{9E}/2 + \varepsilon_{9E} + \Delta_{13E}/2 + \varepsilon_{13E}$
e_F	$\varepsilon_{2F} + \Delta_{2F}/2 - \delta_{5F}/2 + \varepsilon_{5F}$
e_G	$-\delta_{10G}/2 + \varepsilon_{10G} + \Delta_{13G}/2 + \varepsilon_{13G}$
e_H	$\varepsilon_{3H} + \Delta_{3H}/2 - \delta_{5H}/2 + \varepsilon_{5H}$
e_K	$-\delta_{11K}/2 + \varepsilon_{11K} + \Delta_{13K}/2 + \varepsilon_{13K}$
e_L	$\varepsilon_{4L} + \Delta_{4L}/2 - \delta_{6L}/2 + \varepsilon_{6L}$
e_M	$-\delta_{12M}/2 + \varepsilon_{12M} + \Delta_{13M}/2 + \varepsilon_{13M}$
e_N	ε_{6N}
e_1	$-\tau_{1D}/2 + \eta_{1D}$
e_2	$-\tau_{2F}/2 + \eta_{2F}$
e_3	$-\tau_{3H}/2 + \eta_{3H}$
e_4	$-\tau_{4L}/2 + \eta_{4L}$

4.3 Analysis of static misalignment

A first requirement to be controlled on the gear train is the alignment of the input and output shafts connected with external devices. In general cases, the position of each shaft may have to be separately controlled with respect to a common set of features on the housing, e.g. a mating plane and a centering bore. For the sake of simplicity, the relative position of the two shafts will be analyzed considering the two distinct requirements of translational and rotational alignment.

The translational error is the radial displacement between points A and N. In the equivalent static model shown in Fig. 3a, two opposing forces F are applied to the two points along X. These have effects on two of the three beams, because gear meshes do not transmit shaft deflections due to radial tooth clearances. The support reactions are calculated by solving the static model. All the forces are then divided by F to get the composite sensitivities:

$$s_A = 1, \quad s_B = 1 + a/c, \quad s_C = a/c$$

$$s_K = a/2b, \quad s_M = 1 + a/2b, \quad s_N = 1$$

The sensitivities of the errors on part features can now be calculated by the expressions in Tab. 2. For example, the following sensitivities are found for the errors on the housing bore diameter in B (Δ_{13B}) and on the corresponding bearing outer-ring diameter (δ_{7B}):

$$s(\Delta_{13B}) = s_B \cdot \partial e_B / \partial \Delta_{13B} = s_B/2 = (a+c)/2c$$

$$s(\delta_{7B}) = s_B \cdot \partial e_B / \partial \delta_{7B} = -s_B/2 = -(a+c)/2c$$

For a geometric check, it can be noted that both a larger bore on the housing and a smaller outer ring on the bearing in B involve an increased radial clearance between them. The input shaft is thus allowed a larger rotation angle about the other support in C, and its end journal in A moves further away from its nominal position. The absolute value of the two sensitivities comes from the radial clearance (half the diametral clearance) amplified by lever effect from B to A.

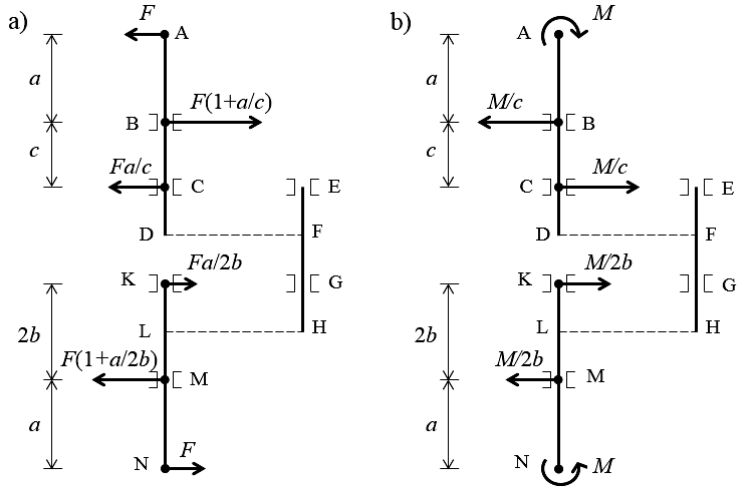

Fig. 3: Force analysis for shaft misalignment: a) translational, b) rotational

The rotational error is the angular displacement between A and N. In the static model of Fig. 3b, opposing torques M are applied to the two points. The support reactions are calculated and divided by M to get the following sensitivities:

$$s_B = 1/c, \quad s_C = 1/c$$

$$s_K = 1/2b, \quad s_M = 1/2b$$

The torques at A and N are also divided by M yielding unit sensitivities for the angular errors θ_A and θ_N at the two points. These errors are not directly toleranced, but their maximum values are related to the position errors by the following expressions:

$$\theta_A = e_A/a, \quad \theta_N = e_N/a$$

This gives two additional sensitivities on the angular misalignment:

$$s_A = 1/a, \quad s_N = 1/a$$

The sensitivities of part feature errors are calculated as explained for the translational error. The sensitivities of the same two errors considered above are

$$s(\Delta_{13B}) = s_B/2 = 1/2c$$

$$s(\delta_{7B}) = -s_B/2 = -1/2c$$

and can be immediately checked by geometric reasoning.

4.4 Analysis of center distance errors

The variation of the center distance of meshing gears must be controlled in order to avoid radial tooth jamming, reduction of contact ratio, and deviations on the nominal pressure angle with possible overloading and vibration. The actual center distance depends on the pitch circle runout of the gears as well as on the eccentricities of mounting parts. For the reference case, the requirement will be separately analyzed for meshes 1-2 and 3-4. In both cases, the center distance error is the relative displacement along X of the two points corresponding to the gear sections in the skeletal structure.

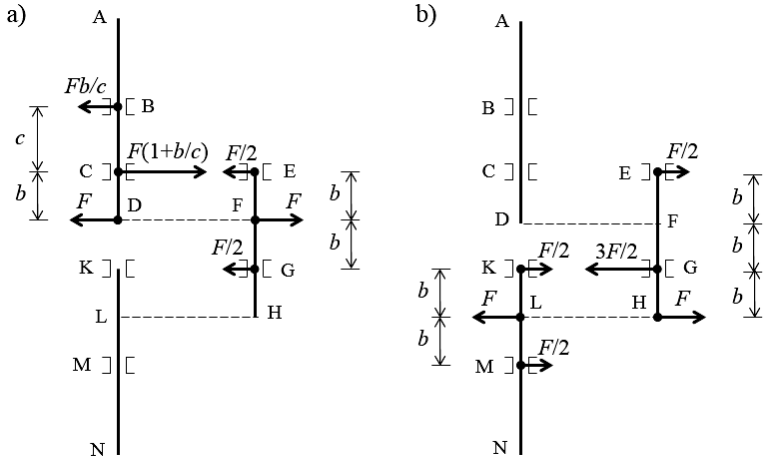

Fig. 4: Force analysis for center distance errors: a) mesh 1-2, b) mesh 3-4

In the first static model, shown in Fig. 4a, two opposing forces F are applied horizontally to points D and F. As previously noted, these loads are equilibrated by support reactions on the same two beams, while the third beam remains unloaded. The reactions are calculated and divided by F to get the composite sensitivities:

$$s_B = b/c, \quad s_C = 1 + b/c, \quad s_D = 1$$

$$s_E = 1/2, \quad s_F = 1, \quad s_G = 1/2$$

Again, the expressions in Tab. 2 lead to the sensitivities related to individual features. For example:

$$s(\varepsilon_{1D}) = s_D \cdot \partial e_D / \partial \varepsilon_{1D} = s_D = 1$$

Expectedly, a given amount of pitch circle runout ε_{1D} on pinion 1 causes an equal amount of radial displacement with respect to the toothed surface of gear 2.
In the second static model, shown in Fig. 4b, the same loads are applied to points H and L. Solving the free-body diagrams and dividing the forces by F, the following composite sensitivities result:

$$s_E = 1/2, \quad s_G = 3/2, \quad s_H = 1$$

$$s_K = 1/2, \quad s_L = 1, \quad s_M = 1/2$$

Among feature errors, the highest sensitivities are related to the housing bore in G (diameter error Δ_{13G}, position error ε_{13G}):

$$s(\Delta_{13G}) = s_G \cdot \partial e_G / \partial \Delta_{13G} = s_G / 2 = 3/4$$

$$s(\varepsilon_{13G}) = s_G \cdot \partial e_G / \partial \varepsilon_{13G} = s_G = 3/2$$

As it can also be noted for shaft misalignment and consistently with practical experience, meshing precision thus seems relatively critical for outboard gears.

4.5 Analysis of backlash

Backlash is a key issue for gear drives of servomotors and fine mechanisms, which are subject to motion reversals and thus to possible lost motion caused by angular tooth clearances. To avoid tooth jamming and allow thermal expansion and lubricant space, a deliberate backlash is created by a small allowance on tooth thickness. Random deviations from average backlash are due to several error sources, including tooth thickness and profile errors, pitch circle runouts, and eccentricities of mounting parts. Considering the stackup of backlashes over the stages of a gear train, this functional requirement may involve a large set of tolerances, whose contributions to total error are especially difficult to analyze.
For the reference case, the static analogy will be used to evaluate the angular backlash on the output shaft once the rotation of the input shaft is restrained. The equivalent static model, shown in Fig. 5, includes the skeletal structure and the pitch circles. The load applied to the structure is an axial torque M on point N, while point A is clamped against axial rotation. The solution of the static model involves a larger set of equilibrium conditions than in previous analyses (translations along X and Z, rotations about Y and Z). These yield the components of reaction and internal forces along X and Z, which are summed vectorially and divided by M, thus obtaining the following set of composite sensitivities:

$$s_A = \frac{r_1 r_3}{r_2 r_4}, \quad s_B = \frac{r_3 b}{r_2 r_4 c \cos\varphi}, \quad s_C = \frac{2 r_3 (b+c)}{r_2 r_4 c \cos\varphi}, \quad s_D = \frac{r_3 \tan\varphi}{r_2 r_4}$$

$$s_E = \frac{1}{2 r_4 \cos\varphi} \sqrt{\frac{r_3^2}{r_2^2} + 2\frac{r_3}{r_2}\cos 2\varphi + 1}, \quad s_F = \frac{r_3 \tan\varphi}{r_2 r_4}, \quad s_G = \frac{1}{2 r_4 \cos\varphi} \sqrt{\frac{r_3^2}{r_2^2} - 6\frac{r_3}{r_2}\cos 2\varphi + 9}, \quad s_H = \frac{\tan\varphi}{r_4}$$

$$s_K = \frac{1}{2 r_4 \cos\varphi}, \quad s_L = \frac{\tan\varphi}{r_4}, \quad s_M = \frac{1}{2 r_4 \cos\varphi}, \quad s_N = 1$$

$$s_1 = \frac{r_3}{r_2 r_4}, \quad s_2 = \frac{r_3}{r_2 r_4}, \quad s_3 = \frac{1}{r_4}, \quad s_4 = \frac{1}{r_4}$$

where φ is the pressure angle of all the gears.
The two dimensionless sensitivites (s_A and s_N) are related to the angular errors on shaft ends, arising from possible clearances on keyways that are not considered in this example. The remaining composite sensitivities have dimensions of reciprocal lengths, i.e. transform linear dimensions into angles. Consistently with known properties of backlash, the main contributions are on the output shaft, where eccentricities and

radial clearances cause a considerable variation of the center distance of mesh 3-4. The following sensitivities are found for the errors on the toothed surface of gear 4:

$$s(\varepsilon_{4L}) = s_L \cdot \partial e_L / \partial \varepsilon_{4L} = s_L = \frac{\tan\varphi}{r_4}$$

$$s(\tau_{4L}) = s_4 \cdot \partial e_4 / \partial \tau_{4L} = -s_4/2 = -\frac{1}{2r_4}$$

$$s(\eta_{4L}) = s_4 \cdot \partial e_4 / \partial \eta_{4L} = s_4 = \frac{1}{r_4}$$

The above expressions multiplied by r_4 give the sensitivities of the same errors on the linear backlash of mesh 3-4. Consistently with known results, it can be recognized that pitch circle runout ε_{4L} creates an equal increase of peak center distance, which in turn influences the linear backlash through a factor $\tan\varphi$. A reduction of tooth thickness $-\tau_{4L}$ and a tooth profile error η_{4L} have similar effects, without the multiplicative factor as they are defined along the pitch circle arc.

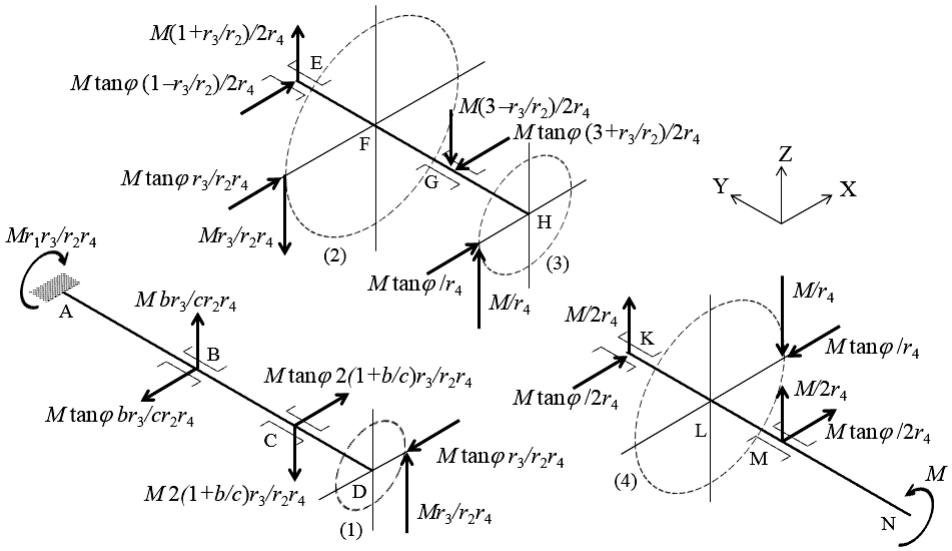

Fig. 5: Force analysis for backlash

5 Results

The sensitivities calculated in Section 4 allow to estimate the variation of each functional requirement from a given set of part tolerances, along with the contribution of each tolerance to total variation. Results for the example are presented below under the assumptions listed in Tab. 3 about dimensions and tolerances. For diameters and tooth thicknesses, an allowance (i.e. average deviation from nominal fitting dimension) equal to half the tolerance is assumed in order to ensure a locational clearance fit with the mating feature. With the exception of bearings, diameter and positional tolerances are set to a common value to allow a direct appreciation of error stackup. In practical applications, this would be done at the first iteration of an allocation procedure where the tolerances with the largest contributions are later reduced in the attempt to satisfy given functional specifications at lower cost.

The variation of a requirement y is expressed as a mean Y_0 and a tolerance T_y:

$$Y_0 = \sum_i |s_i| \mu_i \,, \quad T_y = \sqrt{\sum_i s_i^2 T_i^2}$$

where the summations are extended to each single error listed in Tab. 1, whose tolerance T_i and allowance μ_i are given, and whose sensitivity s_i is calculated by static analogy. Tolerance T_y has the same meaning of part

tolerances, e.g. corresponds to ±3 times the standard deviation of the normally distributed error δy. The equations assume the statistical independence of feature errors, although some eccentricities are actually the sum of independently phased periodic errors with the same frequency (corresponding to shaft rotation); corrections for such issue are available in literature [5].

Tab. 3: Assumptions about dimensions and tolerances

Type	*Data*
Pitch circle radii [mm]	$r_1 = 24$, $r_2 = 60$, $r_3 = 36$, $r_4 = 48$
Pressure angle	$\varphi = 20°$
Axial distances [mm]	$a = 100$, $b = 60$, $c = 80$
Diameter and tooth tolerances [mm]	$T_d = T_D = T_t = 0.02$ (bearings: 0.005)
Diameter and tooth allowances [mm]	$\mu_d = \mu_D = \mu_t = 0.01$ (bearings: 0.0025)
Positional tolerances [mm]	$T_e = T_E = 0.02$ (bearings: 0.005)

With the same notation, the percentage contribution of each tolerance to the variation of y is calculated as

$$c_{iy} = \frac{s_i^2 T_i^2}{T_y^2}$$

In what follows, the total variation will be presented as $Y_0 \pm T_y/2$, and the error causes will possibly be aggregated according to some criterion (type of tolerance, type of component, location) by summing their percentage contributions.

5.1 Shaft misalignment

Translational misalignment is estimated at 0.040 ± 0.040 mm. Fig. 6a shows the percentage contributions aggregated by feature type: bearings give a marginal contribution due to their high manufacturing accuracy; housing bores are especially critical (82% of total error), while shaft journals have a minor impact (12%) due to their small number. Fig. 6b details the contributions of individual tolerances, showing that the two most critical housing bores are the ones closer to the end journals on the input shaft (31%) and on the output shaft (21%); the difference is related to the shorter span of the supports on the input shaft, which causes a higher amplification of eccentricities.

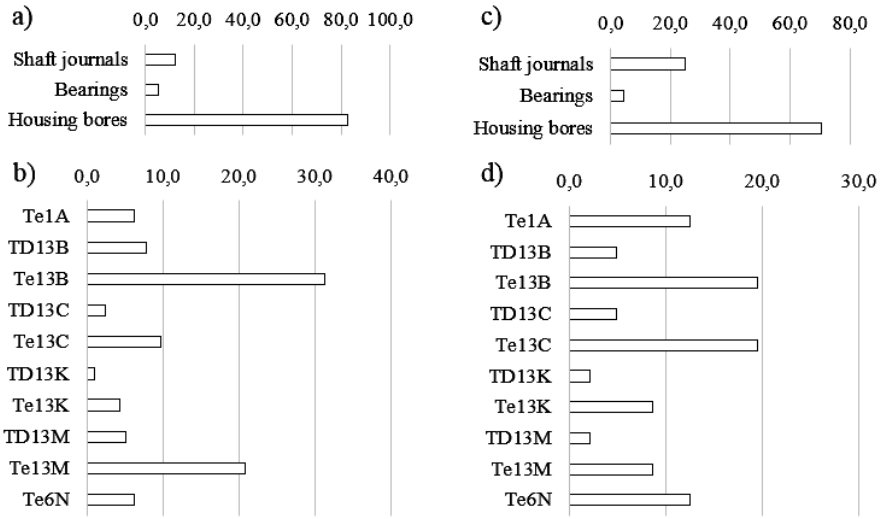

Fig. 6: Contributions to shaft misalignment: translational error, a) by feature type, b) individual tolerances; rotational error, c) by feature type, d) individual tolerances

Rotational misalignment is estimated at 0.015 ± 0.015 degrees. As shown in Fig. 6c-d, housing bores account for most of the variation (71%), especially at the input side due to the closer supports. Not entirely negligible is the influence of the eccentricities of shaft end journals (25%), with equal contributions from the input and output side due to the equal journal lengths.
As an insight for tolerance allocation, it can be noted again that positional errors have double sensitivities compared to diameter errors on the same features. For housing bores, this magnifies the contribution of positional error to both translational and rotational misalignment. To reduce total variation, positional tolerances should be reduced with equal diameter tolerances; such choice would probably require a different layout of the housing where all the boring operations could be done in the same setup and a rigid boring tool could freely approach the machining areas.

5.2 Center distance errors

Center distance errors are estimated at 0.027 ± 0.030 mm for mesh 1-2 and 0.042 ± 0.033 mm for mesh 3-4. As shown in Figs. 7a-b, pitch circle runouts give a minor contribution to total variation (22% and 19% for the two gear pairs). More critical are the errors on non-meshing features, such as housing bores (57% and 49%) and mating features between shafts and gears (adding up to 17% and 29%); the different contributions can be explained considering that the integral pinion in the first mesh avoids additional errors due to mounting features. In Figs. 7c-d, a first consideration is that pitch circle runouts on meshing gears give equal contributions to total variation. Moreover, the most critical features are located at the sections next to outboard gears (C and G), suggesting that such arrangements of supports should be avoided for the sake of precision. As already noted, a reduction of positional tolerances on housing bores would be mostly beneficial, while tighter diameter tolerances would give little improvement. Again, this choice would create difficulties in manufacturing due to approach limitations for the boring tool. Redesigning the housing in multiple parts to allow an axial fitting of shaft subassemblies would probably improve the control of center distances despite the additional error sources due to the mating features at housing part connections.

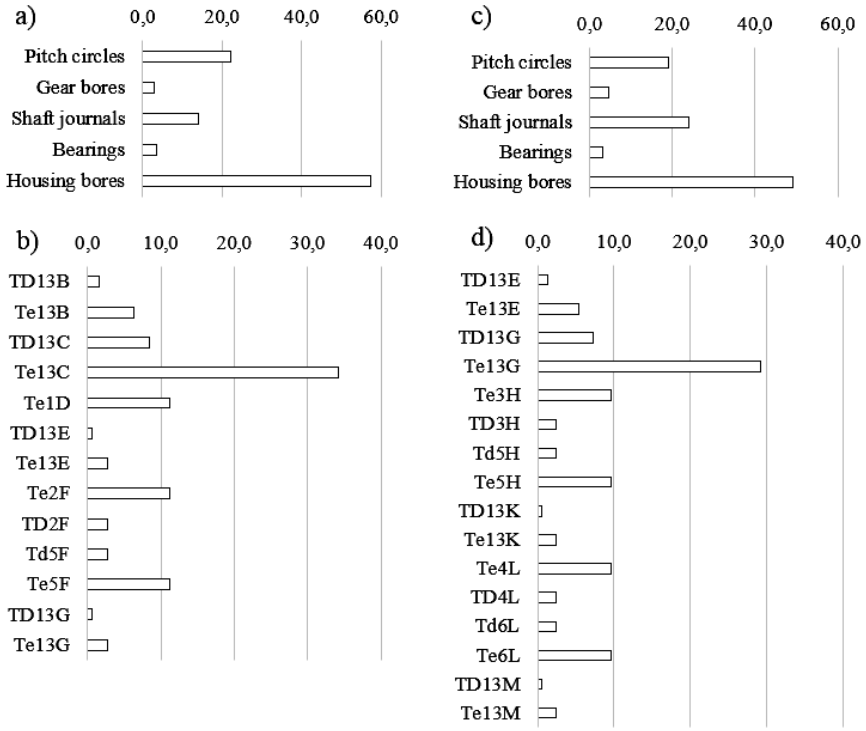

Fig. 7: Contributions to center distance errors: mesh 1-2, a) by feature type, b) individual tolerances; mesh 3-4, c) by feature type, d) individual tolerances

5.2 Backlash

Angular backlash is estimated at 1.15 ± 0.66 mrad; the lower limit avoids tooth jamming, while the upper limit would corresponds to a backlash within 0.1% of driven hub diameter. Fig. 8a confirms the major role (55% of total variation) of housing bore errors, which cause center distance errors with an indirect effect on backlash. The second most important source of backlash (33%) is related to gear teeth, while the remaining features (including pitch circles) individually have a negligible influence. The results in Fig. 8b seem to contradict the well-known fact that backlash at the output shaft is mostly determined by the last stages of a reduction gear unit. Although the calculation correctly accounts for the effect of velocity ratio, the output shaft subassembly in the example has the advantage of a higher rigidity, as it does not include outboard gears (which turns out to be a good choice).

The contributions of individual tolerances are shown in Figs. 8c-d-e for the three shaft subassemblies. Once again, positional errors of housing bores are especially critical at the sections close to outboard gears, with an obvious prevalence of the intermediate shaft (point G) with respect to the input shaft (point C). Tooth errors have a sharply increasing influence from the first to the second mesh; profile errors give a larger contributions than thickness errors if, as assumed as a baseline, equal tolerances are specified for the two characteristics. As an improvement, tooth profile tolerances should be reduced for gears 3 and 4 at least; this choice would balance the contribution of the different tooth errors with a slight reduction of total backlash.

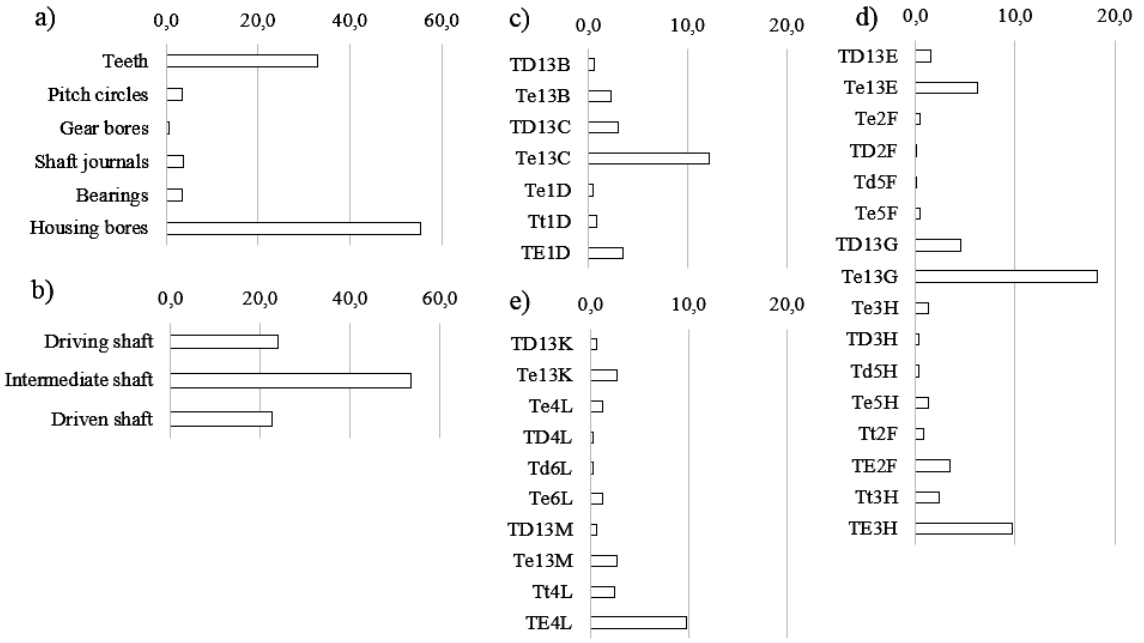

Fig. 8: Contributions to backlash: a) by feature type, b) by shaft; individual tolerances on c) input shaft, d) intermediate shaft, e) output shaft

6 Further application

The example discussed so far has allowed a straightforward application of the static analogy due to the simple force flow created by spur gears and radial bearings. More complex gear train designs may require careful attention in defining the static model, choosing the external forces, and matching reaction forces with toleranced part features. An example of different configuration in given below.

For the two-stage reduction unit with helical gears in Fig. 9a, the angular backlash at the output shaft is to be analyzed. The shaft and the bearings are radially assembled into a split housing, and thrust covers are fit to bores in the housing to axially restrain the bearings where indicated by arrows. As in the main example, the equivalent static model in Fig. 9b includes three beams corresponding to the shafts (input, intermediate, output) and the pitch circles of the gears (1, 2, 3, 4). An axial torque *M* acts at the end of the output shaft,

while the input shaft is rotationally restrained. Focusing on the input shaft subassembly, the static model boils down to a single beam with gear 1 mounted at point C at distances *a* and *b* from supports A and B, the former providing registration against axial displacements.

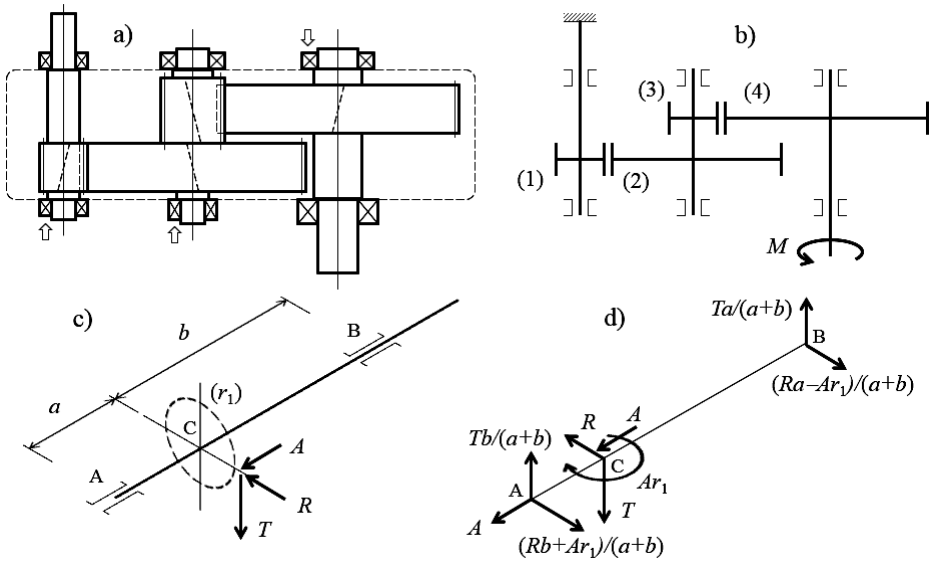

Fig. 9: Backlash on parallel helical gears: a) assembly, b) static model, c) forces on input shaft, d) solution

Fig. 9c shows the components of the meshing force on gear 1. In addition to tangential force *T* and radial force *R*, there is an axial force *A* acting at distance r_1 from shaft center (r_1 being the pitch radius of pinion 1); the three forces are readily calculated from known geometric relations regarding helical gears:

$$T = \frac{Mr_3}{r_2 r_4}$$

$$A = T\tan\psi = \frac{Mr_3}{r_2 r_4}\tan\psi$$

$$R = T\frac{\tan\varphi_n}{\cos\psi} = \frac{Mr_3}{r_2 r_4}\frac{\tan\varphi_n}{\cos\psi}$$

where r_i is the pitch radius of gear *i*, and φ_n and ψ are the normal pressure angle and the helix angle of the pinion. Fig. 9d shows the free-body diagram of the input shaft.

The tangential force on the pitch circle divided by *M* gives the composite sensitivity at the pitch point:

$$s_1 = \frac{r_3}{r_2 r_4}$$

It transforms displacements along the pitch circle arc into contributions to angular backlash. From s_1, the sensitivities of tooth thickness and tooth profile errors can be derived by applying the appropriate factors (−1/2 and 1).

Dividing the resultant radial forces by *M* gives three composite sensitivities at points A, B and C:

$$s_A = \frac{r_3}{r_2 r_4}\frac{b}{a+b}\sqrt{1+\left(\frac{\tan\varphi_n}{\cos\psi}+\frac{r_1}{b}\tan\psi\right)^2}$$

$$s_B = \frac{r_3}{r_2 r_4}\frac{a}{a+b}\sqrt{1+\left(\frac{\tan\varphi_n}{\cos\psi}-\frac{r_1}{a}\tan\psi\right)^2}$$

$$s_C = \frac{r_3}{r_2 r_4}\sqrt{1+\left(\frac{\tan\varphi_n}{\cos\psi}\right)^2}$$

They transform radial displacements into contributions to angular backlash. At the supports, s_A and s_B determine the sensitivites of the diameter tolerances on bearing outer rings and housing bores (respectively with factor −1/2 and 1/2), and on the position errors on the same features (with factor 1). For the pinion, s_C determines the sensitivity of the tolerance on pitch circle runout (with factor 1).
The torque in C divided by M gives a further composite sensitivity in C:

$$s_{C2} = \frac{r_1 r_3}{r_2 r_4}\tan\psi$$

which is dimensionless and represents the contribution of an angular displacement about an axis normal to the shaft. The cause of such rotation is the angular misalignment between the pitch circle and the shaft journal at C (referred to shaft journals at A and B), whose maximum value is equal to the runout divided by w_1 (width of the pinion). A term equal to s_{C2}/w_1 is thus added to the sensitivity of pitch circle runout.
Lastly, the compressive force between A and C gives the sensitivity

$$s_{AC} = -\frac{r_3}{r_2 r_4}\tan\psi$$

which represent the contribution of an axial displacement of the shaft. The cause of such displacement is the possible axial clearance between the bearing and the cover in A. In operation, such clearance is equal to zero because the axial force on the pinion pushes the bearing against the cover without creating additional backlash; therefore, s_{AC} does not correspond to any tolerance on part features. If the unit were subject to motion reversals, the axial clearance in B would also have to be avoided, e.g. by a preload or a shim pack. Axial forces could also play a role for bevel gears depending on the bearing arrangement.

7 Conclusions

A gear train may require a tight control of several geometric characteristics, each depending in a possibly complex way on many features on gears and mounting parts. The impact of individual tolerances on the variation of the functional requirements can be evaluated through a few methods available in literature. However, they either involve complex mathematical procedures or do not take full account of the detailed assembly layout and dimensions. The method based on static analogy, previously developed for generic assemblies and here proposed with some adaptations in the context of gear systems, has the potential for simplifying tolerance analysis for this class of mechanisms due to the following reasons:

- it treats different requirements (shaft alignment, center distances, backlash) with a similar formulation and geometric model;
- it converts tolerance analysis problems into equivalent force analysis problems, which are easily solved through free-body diagrams due to the static determinacy of gear systems;
- it divides the analysis into two hierarchical levels, the first one using force analysis to find aggregate results for each section of the transmission (composite sensitivities), the second one allocating the aggregate results to the part features located in the same sections (sensitivities of part tolerances);
- it uses known equations giving the meshing forces between gears of various types (spur, helical, bevel);
- it can deal with complex gear trains, where a similar static analysis with the actual operating loads is needed for the structural design of gears, shafts and bearings.

The application of the method to a basic example has given correct results in comparison to geometric reasoning. As demonstrated on a further application, the static analogy is suitable to a wider range of gear

train configurations; a further validation will be needed for more complex cases in comparison to existing tolerance analysis methods, possibly supported by computer-aided tools.

Future developments will also aim at overcoming some current limitations of the method. Specifically, an equivalent static model should be developed for the transmission error, which cannot be analyzed by the method in its current formulation. Moreover, the pre-selection of part features for different functional requirements should rely upon a more structured procedure, which could avoid the subjective judgement now required for a correct application of the method.

Other limitations that will have to be released are related to thermal expansion and bending deflection, which are currently neglected by the method. Since, as it has been mentioned, the meshing conditions of involute gears are robust with respect to variation of center distance, including the deformations in the analysis would not violate the basic assumption of statical determinacy. The extension would therefore require a separate evaluation of the thermal and elastic effects, to be combined appropriately with the sensitivities of manufacturing errors.

A further objective is the development of a software tool for the tolerance analysis of gear trains based on the static analogy. As an alternative to a full integration with CAD modelers, the tool should probably provide an interactive construction of a geometric representation of the gear train at a level of detail consistent with the required input data (layout, diameters, axial dimensions, and tolerances). For a given range of allowable configurations, the construction and resolution of the free body diagrams could easily be automated. For the same tasks, procedures based on the use of commercial software packages for finite element analysis might also be devised.

Funding

This research did not receive any specific grant from funding agencies in the public, commercial, or not-for-profit sectors.

References

[1] P.K. Singh, P.K. Jain, S.C. Jain, Important issues in tolerance design of mechanical assemblies. Part 1: tolerance analysis, Proc. Inst. Mech. Eng. Part C 223 (2009) 1225-1247.

[2] W. Polini, Geometric tolerance analysis, in: B.M. Colosimo, N. Senin (Eds.), Geometric tolerances, Springer, London, 2011, pp. 39-68.

[3] B. Schleich, S. Wartzack, A quantitative comparison of tolerance analysis approaches for rigid mechanical assemblies, Procedia CIRP 43 (2016) 172-177.

[4] S.P. Radzevich, Dudley's Handbook of practical gear design and manufacture, 2nd Ed., CRC Press, Boca Raton (2012).

[5] G.W. Michalec, Precision gearing: theory and practice, John Wiley & Sons, New York (1966).

[6] G. Goch, Gear metrology, CIRP Annals 52-2 (2003) 659-695.

[7] G. Goch, K. Ni, Y. Peng, A. Guenther, Future gear metrology based on areal measurements and improved holistic evaluation, CIRP Annals Manuf. Technol. 66 (2017) 469-474.

[8] J.Y. Dantan, J. Bruyere, C. Baudouin, L. Mathieu, Geometrical specification model for gear: expression, metrology and analysis, CIRP Annals 56-1 (2007) 517-520.

[9] J.Y. Dantan, J.P. Vincent, G. Goch, L. Mathieu, Correlation uncertainty: application to gear conformity, CIRP Annals Manuf. Technol. 59 (2010) 509-512.

[10] M. Zhang, Z.Y. Shi, L. Mathieu, N. Anwer, J. Yang, Geometric product specification of gears: the GeoSpelling perspective, Procedia CIRP 27 (2015) 90-96.

[11] F.L. Litvin, Development of gear technology and theory of gearing, NASA Ref. Pub. 1406 (1998).

[12] F.L. Litvin, J. Lu, D.P. Townsend, M. Howkins, Computerized simulation of meshing of conventional helical involute gears and modification of geometry, Mech. Mach. Theory 34 (1999) 123-147.

[13] F.L. Litvin, M. De Donno, A. Peng, A. Vorontsov, R.F. Handschuh, Integrated computer program for simulation of meshing and contact of gear drives, Comput. Methods Appl. Mech. Engrg. 181 (2000) 71-85.
[14] F.L. Litvin, G.I. Sheveleva, D. Vecchiato, I. Gonzalez-Perez, A. Fuentes, Modified approach for tooth contact analysis of gear drives and automatic determination of guess values, Comput. Methods Appl. Mech. Engrg. 194 (2005) 2927-2946.
[15] R.T. Tseng, C.B. Tsay, Contact characteristics of cylindrical gears with curvilinear shaped teeth, Mech. Mach. Theory 39 (2004) 905-919.
[16] D. Vecchiato, Tooth contact analysis of a misaligned isostatic planetary gear train, Mech. Mach. Theory 41 (2006) 617-631.
[17] A. Bracci, M. Gabiccini, A. Artoni, M. Guiggiani, Geometric contact pattern estimation for gear drives, Comput. Methods Appl. Mech. Engrg. 198 (2009) 1563-1571.
[18] C.H. Lin, Z.H. Fong, Numerical tooth contact analysis of a bevel gear set by using measured tooth geometry data, Mech. Mach. Theory 84 (2015) 1-24.
[19] J. Bruyère, J.Y. Dantan, R. Bigot, P. Martin, Statistical tolerance analysis of bevel gear by tooth contact analysis and Monte Carlo simulation, Mech. Mach. Theory 42 (2007) 1326-1351.
[20] J.Y. Dantan, J. Bruyere, J.P. Vincent, R. Bigot, Vectorial tolerance allocation of bevel gear by discrete optimization, Mech. Mach. Theory 43 (2008) 1478-1494.
[21] J.P. Vincent, J.Y. Dantan, R. Bigot, Virtual meshing simulation for gear conformity verification, CIRP J. Manuf. Sci. Technol. 2 (2009) 35-46.
[22] B. Schleich, S. Wartzack, Tolerance analysis of rotating mechanism based on skin model shapes in discrete geometry, Proc. CIRP Conf. on Comput. Aided Tolerancing, Hangzhou, China (2014).
[23] B. Schleich, S. Wartzack, A discrete geometry approach for tolerance analysis of mechanism, Mech. Mach. Theory 77 (2014) 148-163.
[24] B. Schleich, S. Wartzack, Tolerance analysis of rotating mechanism based on skin model shapes in discrete geometry, Procedia CIRP 27 (2015) 10-15.
[25] J. Kim, W.J. Song, B.S. Kang, Stochastic approach to kinematic reliability of open-loop mechanism with dimensional tolerance, Appl. Math. Model. 34 (2010) 1225-1237.
[26] W. Kim, H.H. Yoo, J. Chung, Dynamic analysis for a pair of spur gears with translational motion due to bearing deformation, J. Sound Vibration 329 (2010) 4409-4421.
[27] Q. Chen, Y. Ma, S. Huang, H. Zhai, Research on gears' dynamic performance influenced by gear backlash based on fractal theory, Appl. Surf. Sci. 313 (2014) 325-332.
[28] W. Guangjian, C. Lin, Y. Lin, Z. Shuaidong, Research on the dynamic transmission error of a spur gear pair with eccentricities by finite element method, Mech. Mach. Theory 109 (2017) 1-13.
[29] F.L. Litvin, R.N. Goldrich, J.J. Coy, E.V. Zaretsky, Kinematic precision of gear trains, NASA Tech. Memorandum 82887 (1982).
[30] C.D. Carr, A comprehensive method for specifying tolerance requirements for assemblies, ADCATS Report 93-1, Brigham Young University, 1993.
[31] K.W. Chase, A.R. Parkinson, A survey of research in the application of tolerance analysis to the design of mechanical assemblies, Res. Eng. Des. 3 (1991) 23-37.
[32] J.W. Wittwer, K.W. Chase, L.L. Howell, The direct linearization method applied to position error in kinematic linkages, Mech. Mach. Theory 39 (2004) 681-693.
[33] B.M. Imani, M. Pour, Tolerance analysis of flexible kinematic mechanism using DLM method, Mech. Mach. Theory 44 (2009) 445-456.
[34] D.J.A. Villaroman, 2D tolerance analysis of truss-like assembly structure, Study paper 09564798, Hong Kong University of Science and Technology, 2013.
[35] J. Stuppy, H. Meerkamm, Tolerance analysis of a crank mechanism by taking into account different kinds of deviation, Proc. CIRP Conf. on Comput. Aided Tolerancing, Annecy, France (2009).

[36] M. Walter, T. Sprügel, S. Wartzack, Tolerance analysis of systems in motion taking into account interactions between deviations, Proc. Inst. Mech. Eng. Part B 227 (2013) 709-719.
[37] Z. Shi, Synthesis of mechanical error in spatial linkages based on reliability concept, Mech. Mach. Theory 32 (1997) 255-259.
[38] Z. Shi, X. Yang, W. Yang, Q. Cheng, Robust synthesis of path generating linkages, Mech. Mach. Theory 40 (2005) 45-54.
[39] R.S. Hartenberg, J. Denavit, Kinematic synthesis of linkages, McGraw-Hill, New York, 1964.
[40] S. Dobowsky, F. Freudenstein, Dynamic analysis of mechanical systems with clearances, Part 1: Formulation of dynamic model, ASME J. Eng. Ind. 90 (1971) 305-316.
[41] R.E. Garret, A.S. Hall, Effects of tolerance and clearance in linkage design, ASME J. Eng. Ind. 91 (1969) 198-202.
[42] L. Joskowicz, Mechanism comparison and classification for design, Res. Eng. Des. 1 (1990) 149-166.
[43] L. Joskowicz, E. Sacks, Computational kinematics, Artif. Intell. 51 (1991) 381-416.
[44] L. Joskowicz, E. Sacks, V. Srinivasan, Kinematic tolerance analysis, Comput. Aided Des. 29 (1997) 147-157.
[45] E.P. Sacks, L. Joskowicz, R. Schultheiss, U. Kinze, Computer-assisted kinematic tolerance analysis of a gear selector mechanism with the configuration space method, Comput. Sci. Tech. Reports, 99-003, Purdue University
[46] J.H. Choi, S.J. Lee, D.H. Choi, Tolerance optimization for mechanisms with lubricated joints, Multibody Syst. Dyn. 2 (1998) 145-168.
[47] S.S. Rao, P.K. Bhatti, Probabilistic approach to manipulator kinematics and dynamics, Reliab. Eng. Syst. Saf. 72 (2001) 47-58.
[48] W. Wu, S.S. Rao, Uncertainty analysis and allocation of joint tolerances in robot manipulators based on interval analysis, Reliab. Eng. Syst. Saf. 92 (2007) 54-64.
[49] W.T. Chang, L.I. Wu, Tolerance analysis and synthesis of cam-modulated linkages, Math. Comput. Model. 57 (2013) 641-660.
[50] U. Kumaraswamy, M.S. Shunmugam, S. Sujatha, A unified framework for tolerance analysis of planar and spatial mechanisms using screw theory, Mech. Mach. Theory 69 (2013) 168-184.
[51] M.J. Tsai, T.H. Lai, Kinematic sensitivity analysis of linkage with joint clearance based on transmission quality, Mech. Mach. Theory 39 (2004) 1189-1206.
[52] M.J. Tsai, T.H. Lai, Accuracy analysis of a multi-loop linkage with joint clearances, Mech. Mach. Theory 43 (2008) 1141-1157.
[53] A. Armillotta, A static analogy for 2D tolerance analysis, Assem. Autom. 34 (2014) 182-91.
[54] A. Armillotta, Force analysis as a support to computer-aided tolerancing of planar linkages, Mech. Mach. Theory 93 (2015) 11-25.
[55] A.H. Chebbi, Z. Affi, L. Romdhane, Prediction of the pose errors produced by joint clearance for a 3-UPU parallel robot, Mech. Mach. Theory 44 (2009) 1768-1783.
[56] C. Innocenti, Kinematic clearance sensitivity analysis of spatial structures with revolute joints, ASME J. Mech. Des. 124 (2002) 52-57.
[57] V. Parenti-Castelli, S. Venanzi, Clearance influence analysis on mechanisms, Mech. Mach. Theory 40 (2005) 1316-1329.
[58] S. Venanzi, V. Parenti-Castelli, A new technique for clearance influence analysis in spatial mechanisms, ASME J. Mech. Des. 127 (2005) 446-455.
[59] A. Pott, M. Hiller, A force based approach to error analysis of parallel kinematic mechanisms, in: J. Lenarčič, C. Galletti (Eds.), On advances in robot kinematics, Springer, Berlin (2004) 293-302.
[60] S.C. Liu, S.J. Hu, Variation simulation for deformable sheet metal assemblies using finite element methods, ASME J. Manuf. Sci. Eng. 119 (1997) 368-374.